Theoretical investigation of synchronous totally asymmetric exclusion processes on lattices with multiple-input–single-output junctions

Ruili Wang,[1,2] Mingzhe Liu,[1] and Rui Jiang[3]
[1]*School of Engineering and Advanced Technology, Massey University, Palmerston North, New Zealand*
[2]*State Key Laboratory for Novel Software Technology, Nanjing University, Nanjing 210093, China*
[3]*School of Engineering Science, University of Science and Technology of China, Hefei 230026, China*
(Received 17 September 2007; revised manuscript received 13 March 2008; published 9 May 2008)

In this paper, we investigate the dynamics of synchronous totally asymmetric exclusion processes on lattices with a multiple-input–single-output (MISO) junction, which consists of m subchains for the input and one main chain for the output. A MISO junction is a type of complex geometry that is relevant to many biological processes as well as vehicular and pedestrian traffic flow. A mean-field approach is developed to deal with the junction that connects the subchains and the main chain. Theoretical results for stationary particle currents, density profiles, and a phase diagram have been obtained. It is found that the phase boundary moves toward the left in the phase diagram with an increase of the number of subchains. The nonequilibrium stationary states, stationary-state phases, and phase boundaries are determined by the boundary conditions of the system as well as by the number of subchains. The density profiles obtained from computer simulations show very good agreement with our theoretical analysis.

DOI: 10.1103/PhysRevE.77.051108 PACS number(s): 05.70.Ln, 02.50.Ey, 05.60.Cd

I. INTRODUCTION

Nonequilibrium transport phenomena have attracted much attention from physicists since physical principles underlying these phenomena can be revealed in terms of phases and phase transitions [1,2]. Totally asymmetric simple exclusion processes (TASEPs) serve as a basic model for nonequilibrium systems and have been widely applied in the study of transport phenomena in chemistry, physics, and biology, for example, particle diffusion through membrane channels [3], the kinetics of synthesis of proteins [4], polymer dynamics in dense media [5], gel electrophoresis [6], intracellular transport of motor proteins moving along cytoskeletal filaments [7], vehicular traffic [1,8] and ant traffic [9].

TASEPs are nonequilibrium one-dimensional lattice models in which particles move along one direction with hard-core interactions. The exact solution of TASEPs has been obtained by using the matrix product ansatz [10] and the Bethe ansatz [11], respectively. Recently, some extensions of TASEPs focus on coupling with Langmuir kinetics [12–21] and/or lattice geometries [22–28], as well as bottleneck-induced transport phenomena as in [29,30]. The authors of Ref. [29] investigated diffusive compartments as bottlenecks in driven transport. They found that, when a diffusive bottleneck is at the boundary of a system, the system cannot reach a maximal current phase; when a diffusive bottleneck is in the interior of the system, the system behavior is dictated by the diffusive bottleneck and has a maximal current defined by the bottleneck. More recently, Ref. [30] introduced a bottleneck phase to describe the phenomenon that the current is independent of boundary conditions.

In this paper, we focus on one special lattice geometry—junctions, which are widely observed in many real physical systems. Those junctions are formed for various reasons. For example, (i) variation of the number of protofilaments on a microtubule *in vitro* [31]; (ii) transport of vesicles in a branching axon or dendrite [32]; (iii) merging of two or more roads; (iv) movement of data through hubs (e.g., switches, routers) on the Internet. This kind of lattice geometry can cause congestion, e.g., in the traffic of molecular motors, vehicles, or data packets. Traffic congestion of molecular motors could lead to some human diseases such as Alzheimer's disease [33] and some neurodegenerative diseases [34]. Vehicular traffic congestion can pollute the environment and increase fuel consumption.

Inspired by this wide range of possible applications, we investigate the dynamics of synchronous (i.e., parallel update) totally asymmetric exclusion processes on lattices with a multiple-input–single-output (MISO) junction (see Fig. 1). The parallel updating procedure has been typically adopted in modeling vehicular and pedestrian traffic [1,8,35]. Multiple inputs exhibit more complex interactions between particles at junction points than two inputs. In reality, it can be observed that several traffic lanes merge into one lane and multiple protofilaments come together to form one protofilament [31]. However, they have not been understood well from the viewpoint of theoretical analysis.

Theoretical calculations, along with a mean-field approximation, are developed. The phase diagram is presented and density profiles are investigated. A phenomenological domain wall theory, based on Refs. [23,36], is used to predict

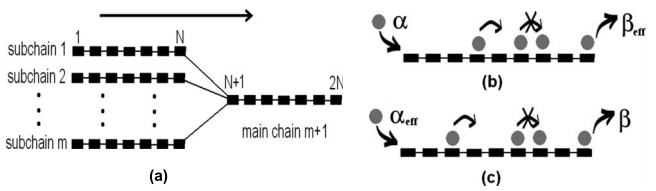

FIG. 1. (a) Schematic diagram of a synchronous TASEP with a MISO junction. Particles move from the left to the right with hard-core exclusion. (b) In a subchain, the injection rate at site 1 and the ejection rate at site N are given by α and β_{eff}, respectively. (c) In the main chain, the injection rate at site $N+1$ and the ejection rate at site $2N$ are given by α_{eff} and β, respectively.

phase boundaries. Computer simulations are also conducted. Note that TASEPs on lattices with Y junctions (e.g., two-input–single-output junctions) with a random updating procedure have been investigated in Ref. [23]. Y junctions can be seen as a special case of multiple-input–single-output junctions.

The paper is organized as follows. In Sec. II, we give a description of a synchronous TASEP model with a MISO junction; theoretical calculations as well as the mean-field approximation are developed. In Sec. III, we analyze the phase boundaries using a phenomenological domain wall theory. In Sec. IV, the results of our theoretical calculations and computer simulations are presented. Finally, we give our conclusions in Sec. V.

II. THE MODEL AND MEAN-FIELD APPROXIMATION

A MISO junction is illustrated in Fig. 1. The system consists of m subchains for input and one main chain (chain $m+1$) for output connected by junction points—sites N on the subchains and site $N+1$ on the main chain. Each subchain and the main chain includes N sites. For simplification, interlane transitions between subchains are not permitted in this paper. Particles are assumed to move from the left to the right.

An occupation variable $\tau_{\ell,i}$ denotes the state of the ith site in the ℓth subchain ($\ell=1,2,\ldots,m$) and the main chain ($\ell=m+1$). $\tau_{\ell,i}=1$ (or $\tau_{\ell,i}=0$) means that site $\tau_{\ell,i}$ is occupied (or empty). The system updates all particles *in parallel* by the following rules (see Fig. 1).

(1) $i=1$. (i) If $\tau_{\ell,1}=0$, a particle enters the system at rate α; or (ii) if $\tau_{\ell,1}=1$ and $\tau_{\ell,2}=0$, then the particle at site $(\ell,1)$ moves into site $(\ell,2)$; or (iii) if both $\tau_{\ell,1}=1$ and $\tau_{\ell,2}=1$, then the particle at site $(\ell,1)$ does not move.

(2) $i=N$. (i) If sites N of k subchains ($1<k\leq m$) are occupied by k particles at the same time, particles have the same priority to hop to site $N+1$. However, only one particle will enter site $N+1$ at any single time step, providing that site $N+1$ is empty. Otherwise (ii) If only one site N of the subchains is occupied by a particle, the particle can directly hop to site $N+1$ providing that site $N+1$ is empty.

(3) $i=2N$. If $\tau_{m+1,2N}=1$, the particle leaves the system with rate β.

(4) $1<i<N$ or $N+1\leq i<2N$. If $\tau_{\ell,i}=1$, the particle can move into site $(\ell,i+1)$ providing $\tau_{\ell,i+1}=0$. Otherwise, the particle cannot move.

Exactly solvable results of a one-dimensional synchronous TASEP have been obtained in Refs. [37,38]. We briefly recall these results, as the solution of our synchronous TASEP with a junction can be derived from them. There are three phases [low density (LD), high density (HD), and maximal current (MC)] and a transition line when $\alpha=\beta$. The MC $J=0.5$ can only be reached at $\alpha=\beta=1$ [38].

(1) When $\alpha<\beta\leq 1$, a low-density phase is obtained with

$$J=\rho,\quad \rho=\rho_1,\quad \rho_1=\frac{\alpha}{1+\alpha},\quad \rho_N=\frac{\alpha}{\beta(1+a)}, \tag{1}$$

where J is the system current, ρ is the bulk density, and ρ_1 (ρ_N) is the particle density at the first (last) site.

(2) When $1\geq\alpha>\beta$, a high-density phase is obtained with

$$J=1-\rho,\quad \rho=\frac{1}{1+\beta},\quad \rho_1=1-\frac{\beta}{\alpha(1+\beta)},\quad \rho_N=\rho. \tag{2}$$

(3) When $\alpha=\beta<1$, a transition line between LD and HD phases is obtained.

(4) When $\alpha=\beta=1$, the maximal current is obtained and $J=0.5$.

Based on the above results, we develop exactly solvable results for TASEPs with a MISO junction. For a MISO junction, as the current is conserved through the system, we have

$$J_1+J_2+\cdots+J_m=J_{m+1},\quad J_1=J_2=\cdots=J_m,$$

$$mJ_\ell=J_{m+1}\leq 0.5, \tag{3}$$

where J_ℓ ($\ell=1,2,\ldots,m$) is the current on the ℓth subchain; J_{m+1} is the current of the main chain.

Each of the m subchains of the MISO junction can be seen as a synchronous TASEP with injection rate α and ejection rate β_{eff}, while the main chain can be seen as a synchronous TASEP with injection rate α_{eff} and ejection rate β. α_{eff} and β_{eff} can be written as

$$\beta_{\text{eff}}=1-\rho_{N+1},\quad \alpha_{\text{eff}}=m\rho_N. \tag{4}$$

These m subchains should have the identical phases when particles on the m subchains merge into the main chain with the same priority. Our computer simulations also support this prediction. Thus, the stationary state of the system can be obtained by combining the possible phases that exist in each of these subchains and the main chain. As each single chain may have three possible phases (LD, HD, and MC), due to the equivalence of these subchains, the number of possible stationary phases of the system is equal to $3^2=9$. In other words, a stationary state can be one of the following nine phases: the (LD, LD), (LD, HD), (LD, MC), (HD, LD), (HD, HD), (HD, MC), (MC, LD), (MC, HD), and (MC, MC) phases.

One can see that three phases cannot exist: (MC, LD), (MC, HD), and (MC, MC). According to Eq. (3), it is impossible for the maximal current phase to exist in a subchain since the maximal possible current in the system is no more than 0.5. Therefore, the number of possible phase combinations is reduced to six, i.e., the (LD, LD), (LD, HD), (LD, MC), (HD, LD), (HD, HD), and (HD, MC) phases.

(1) The (LD, HD) phase. The conditions for this case are as follows:

$$\alpha<\beta_{\text{eff}},\quad \alpha_{\text{eff}}>\beta. \tag{5}$$

From Eqs. (1) and (2), the stationary properties of this phase are given by

$$J_1=\frac{\alpha}{1+\alpha},\quad J_{m+1}=\frac{\beta}{1+\beta},\quad \rho_1=\frac{\alpha}{1+\alpha},$$

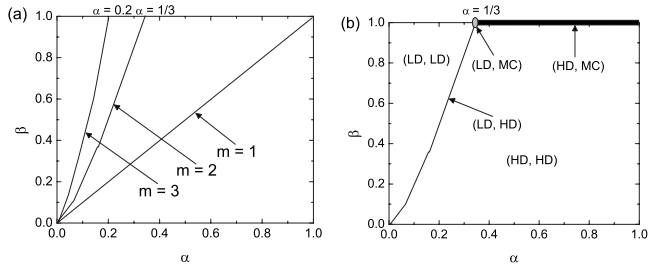

FIG. 2. (a) Phase boundaries (or transition lines) for $m=1,2$, and 3 in a synchronous TASEP with a MISO junction. (b) Phase diagram for $m=2$ in a synchronous TASEP with a MISO junction. The solid line represents the (LD, HD) phase specified by $\alpha=\beta/[m+(m-1)\beta]$ and $\beta<1$; the gray oval corresponds to the (LD, MC) phase specified by $\alpha=1/(2m-1)$ and $\beta=1$; and the black rectangle to the (HD, MC) phase specified by $\alpha>1/(2m-1)$ and $\beta=1$.

$$\rho_N=\frac{\alpha}{\beta_{\text{eff}}(1+\alpha)},\quad \rho_{N+1}=1-\frac{\beta}{\alpha_{\text{eff}}(1+\beta)},\quad \rho_{2N}=\frac{1}{1+\beta}. \tag{6}$$

According to Eq. (3), $mJ_1=J_{m+1}$; we get

$$\alpha=\frac{\beta}{m+(m-1)\beta}. \tag{7}$$

However, α_{eff} and β_{eff} cannot be obtained from the above equations. In other words, we cannot calculate the bulk density through the above equations. The density will be obtained through the domain wall theory in Sec. III. From Figs. 2(a) and 2(b), one can see that $\alpha=\beta/[m+(m-1)\beta]$ (when $\beta<1$) corresponds to the transition line between the (LD, LD) phase and the (HD, HD) phase.

(2) The (LD, MC) phase. This phase corresponds to the following conditions:

$$\alpha<\beta_{\text{eff}},\quad \alpha_{\text{eff}}=\beta=1. \tag{8}$$

According to Eqs. (1) and (3), we obtain

$$\alpha=\frac{1}{2m-1},\quad J_1=\frac{1}{2m},\quad J_{m+1}=0.5. \tag{9}$$

Obviously, $\alpha=1/(2m-1)<1/2$ when $m\geq 2$. That is, Eq. (8) is satisfied. Thus, the (LD, MC) phase can exist in the system when

$$\alpha=\frac{1}{2m-1},\quad \beta=1. \tag{10}$$

Again, we cannot calculate the bulk density through the above equations. The density will also be obtained through domain wall theory in Sec. III. From Figs. 2(a) and 2(b), one can see that the (LD, MC) phase is the transition phase between the (LD, LD), (LD, HD), (HD, HD), and (HD, MC) phases.

(3) The (LD, LD) phase. The following conditions should be satisfied:

$$\alpha<\beta_{\text{eff}},\quad \alpha_{\text{eff}}<\beta. \tag{11}$$

According to Eq. (1), the stationary current and density are given by

$$J_1=\frac{\alpha}{1+\alpha},\quad J_{m+1}=\frac{\alpha_{\text{eff}}}{1+\alpha_{\text{eff}}},\quad \rho_1=\frac{\alpha}{1+\alpha},$$

$$\rho_N=\frac{\alpha}{\beta_{\text{eff}}(1+\alpha)},\quad \rho_{N+1}=\frac{\alpha_{\text{eff}}}{1+\alpha_{\text{eff}}},\quad \rho_{2N}=\frac{\alpha_{\text{eff}}}{\beta(1+\alpha_{\text{eff}})}. \tag{12}$$

Using Eqs. (3) and (4), α_{eff} and β_{eff} are expressed as

$$\alpha_{\text{eff}}=\frac{m\alpha}{1-(m-1)\alpha},\quad \beta_{\text{eff}}=\frac{1-(m-1)\alpha}{1+\alpha}. \tag{13}$$

Since $\alpha_{\text{eff}}\leq 1$ and $\alpha_{\text{eff}}=m\alpha/[1-(m-1)\alpha]$, $\alpha\leq 1/(2m-1)$. Substituting Eq. (13) into Eq. (11), we obtain $\alpha<\sqrt{1+m^2/4}-m/2$ for $\alpha<\beta_{\text{eff}}$, and $\alpha<\beta/[m+(m-1)\beta]$ for $\alpha_{\text{eff}}<\beta$. Since $1/(2m-1)<\sqrt{1+m^2/4}-m/2$ (when $m\geq 2$) and $\beta/[m+(m-1)\beta]\leq 1/(2m-1)$ (as $\beta\leq 1$), the system is in the (LD, LD) phase when

$$\alpha<\frac{\beta}{m+(m-1)\beta},\quad \beta\leq 1. \tag{14}$$

(4) The (HD, HD) phase. The conditions for this case are given by

$$\alpha>\beta_{\text{eff}},\quad \alpha_{\text{eff}}>\beta. \tag{15}$$

The current and density of this phase in a stationary state are

$$J_1=\frac{\beta_{\text{eff}}}{1+\beta_{\text{eff}}},\quad J_{m+1}=\frac{\beta}{1+\beta},\quad \rho_1=1-\frac{\beta_{\text{eff}}}{\alpha(1+\beta_{\text{eff}})},$$

$$\rho_N=\frac{1}{1+\beta_{\text{eff}}},\quad \rho_{N+1}=1-\frac{\beta}{\alpha_{\text{eff}}(1+\beta)},\quad \rho_{2N}=\frac{1}{1+\beta}. \tag{16}$$

From Eqs. (3) and (16), we obtain $\beta_{\text{eff}}=\beta/[m+(m-1)\beta]$. Thus, the system is in the (HD, HD) phase when

$$\alpha>\frac{\beta}{m+(m-1)\beta}. \tag{17}$$

(5) The (HD, MC) phase. The corresponding conditions for this phase are

$$\alpha>\beta_{\text{eff}},\quad \alpha_{\text{eff}}=\beta=1. \tag{18}$$

According to Eqs. (2) and (3), we obtain

$$J_1=\frac{1}{2m},\quad \rho_N=\frac{1}{m},\quad \rho_{N+1}=\frac{2m-2}{2m-1},\quad \beta_{\text{eff}}=\frac{1}{2m-1}. \tag{19}$$

Thus, the (HD, MC) phase can exist in the system when

$$\alpha>\frac{1}{2m-1},\quad \beta=1. \tag{20}$$

(6) The (HD, LD) phase. The conditions of existence for this phase can be written as

$$\alpha > \beta_{\text{eff}}, \alpha_{\text{eff}} < \beta. \tag{21}$$

The corresponding expressions for the stationary current and density are

$$J_1 = \frac{\beta_{\text{eff}}}{1+\beta_{\text{eff}}}, \quad J_{m+1} = \frac{\alpha_{\text{eff}}}{1+\alpha_{\text{eff}}}, \quad \rho_1 = 1 - \frac{\beta_{\text{eff}}}{\alpha(1+\beta_{\text{eff}})},$$

$$\rho_N = \frac{1}{1+\beta_{\text{eff}}}, \quad \rho_{N+1} = \frac{\alpha_{\text{eff}}}{1+\alpha_{\text{eff}}}, \quad \rho_{2N} = \frac{\alpha_{\text{eff}}}{\beta(1+\alpha_{\text{eff}})}. \tag{22}$$

According to Eq. (3), we have

$$\alpha_{\text{eff}} = \frac{m\beta_{\text{eff}}}{1-(m-1)\beta_{\text{eff}}}. \tag{23}$$

From Eqs. (4) and (22), α_{eff} and β_{eff} can be rewritten as follows:

$$\alpha_{\text{eff}} = \frac{m}{1+\beta_{\text{eff}}}, \quad \beta_{\text{eff}} = \frac{1}{1+\alpha_{\text{eff}}}. \tag{24}$$

Substituting Eq. (24) into Eq. (23), we obtain $\alpha_{\text{eff}} = \sqrt{1+m^2/4}+m/2-1$ and $\beta_{\text{eff}} = \sqrt{1+m^2/4}-m/2$. It can be seen that the values of α_{eff} and β_{eff} are determined by the number of subchains m, independent of α and β. This indicates that the (HD, LD) phase cannot be represented in the α-β plane. In other words, the (HD, LD) phase does not exist in the system. In fact, when the subchains are in the high-density phase, particles at site N will hop to site $N+1$ at almost each time step, which leads to $\alpha_{\text{eff}} \approx 1$. Thus, it is impossible for the main chain to maintain the low-density phase.

From the analysis above, one can see that there are five possible phases [(LD, LD), (LD, HD), (LD, MC), (HD, HD), and (HD, MC)] in this system. Figure 2(a) shows the possible phase boundaries $\{\alpha=\beta/[m+(m-1)\beta]\}$ for $m=1$, 2, and 3. With the increase of m, we can predict that the phase boundary moves toward the left in the phase diagram, which means that the low-density area decreases while the high-density area increases. The phase diagram for $m=2$ is also shown in Fig. 2(b). From Fig. 2(b), one can see the following: (i) The (LD, HD) phase corresponds to the transition line between the (LD, LD) phase and the (HD, HD) phase specified by $\alpha=\beta/[m+(m-1)\beta]$ and $0 \le \beta < 1$. (ii) The (LD, MC) phase is the transition phase between the (LD, LD), (LD, HD), (HD, HD) and (HD, MC), phases specified by $\alpha=1/(2m-1)$ and $\beta=1$. Also, note that in the transition from the (LD, LD) phase to the (LD, HD) phase, the density change on the subchains is continuous, while the density change on the main chain is discontinuous. Similarly, in the transition from the (LD, HD) to the (HD, HD) phase, the density change on the subchains is discontinuous, while the density change of the main chain is continuous. Also, for the transition from the (LD, MC) phase to the (HD, MC) phase, the density change on the subchains is discontinuous, while the density profile on the main chain is unchanged.

From the above analysis, we can see the nonequilibrium stationary states, stationary-state phases, and the phase boundaries are determined by the boundary conditions of the system as well as by the number of subchains. In other words, the dynamics of the system is determined by its environment and its own structure.

III. DOMAIN WALL DYNAMICS

A phenomenological domain wall (i.e., shock) theory to explain the phase behavior of a TASEP in a random update procedure with open boundaries was introduced in Ref. [36]. A domain wall is a phase boundary connected by two possible stationary states. The wall can have a random walk through the system with a drift speed defined as follows [36]:

$$V = \frac{J_+ - J_-}{\rho_+ - \rho_-}, \tag{25}$$

where J and ρ are the currents and densities in the two phases; +(−) denotes the phase to the right (left) of the domain wall. When $V>0$, the domain wall moves to the right, while the domain wall travels to the left when $V<0$. For instance, if $\alpha<\beta$ in a TASEP, the domain wall first appears at the left end and will drift to the right later. The wall will pass through the system, which eventually leads to the system being in a low-density stationary state. When $V=0$, it implies that the domain wall has no net drift between two possible phases. In this case, stationary density profiles are linearly increased and the domain wall can exist anywhere with equal probability in the system.

In this paper, the line specified by $\alpha=\beta/[m+(m-1)\beta]$ corresponds to the coexistence of the (LD, LD) and (HD, HD) phases. However, the simple approximation theory may not fully reflect the correlations near the junctions, as indicated in Ref. [23]. The domain wall theory is adopted in order to derive the phase boundary and the density profile in the bulk. This theory has also been used in Ref. [23].

To determine the position of the domain wall in the system, we define x as $x=i/(2N)$, where i is the site index and $2N$ is the length of the system. In the range of $0<x\le 1$, the domain wall moves at rate v_L in the left subsystem (the subchains). In the range of $1<x\le 2$, the domain wall moves at rate v_R in the right subsystem (the main chain); see Fig. 3.

v_L and v_R can be given by utilizing Eq. (25):

$$v_L = \frac{J_L}{\rho_+^L - \rho_-^L}, \quad v_R = \frac{J_R}{\rho_+^R - \rho_-^R}, \tag{26}$$

where

$$J_L = \frac{\alpha}{1+\alpha}, \quad \rho_+^L = \frac{1}{1+\alpha}, \quad \rho_-^L = \frac{\alpha}{1+\alpha}, \quad J_R = \frac{\beta}{1+\beta},$$

$$\rho_+^R = \frac{1}{1+\beta}, \quad \rho_-^R = \frac{\beta}{1+\beta}. \tag{27}$$

As a result, v_L and v_R are rewritten as

$$v_L = \frac{\alpha}{1-\alpha}, \quad v_R = \frac{\beta}{1-\beta}. \tag{28}$$

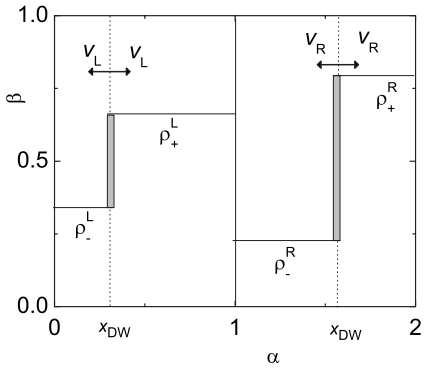

FIG. 3. Schematic diagram of the domain wall dynamics in the (LD, HD) phase. The domain wall moves in the left and right subsystems at rates v_L and v_R, respectively.

As in Ref. [23], q_L (q_R) is denoted as the probability to find the domain wall at any position in the left (right) subsystem. For a special site i in the left (right) subsystem, the probability is obviously equal to q_L/N (q_R/N). Then, at the junction point, we have

$$\frac{v_L q_L}{N} = \frac{v_R q_R}{N}. \tag{29}$$

In addition, the normalized q_L and q_R satisfy

$$q_L + q_R = 1. \tag{30}$$

Combining Eqs. (29) and (30), we obtain

$$q_L = \frac{v_R}{v_L + v_R}, \quad q_R = \frac{v_L}{v_L + v_R}. \tag{31}$$

According to Eq. (28), Eq. (31) implies that

$$q_L = \frac{\beta(1-\alpha)}{\alpha+\beta-2\alpha\beta}, \quad q_R = \frac{\alpha(1-\beta)}{\alpha+\beta-2\alpha\beta}. \tag{32}$$

Accordingly, the probabilities of the domain walls falling in certain zones in the left and right subsystems are also given by

$$\mathrm{Prob}(x_{\mathrm{DW}} > x) = q_L x, \quad 0 < x \le 1, \tag{33}$$

and

$$\mathrm{Prob}(x_{\mathrm{DW}} < x) = q_L + q_R(x-1), \quad 1 < x \le 2. \tag{34}$$

Thus, the density at any position in the system becomes

$$\rho(x)_k = \rho_-^k \mathrm{Prob}(x_{\mathrm{DW}} > x) + \rho_+^k \mathrm{Prob}(x_{\mathrm{DW}} < x), \quad k = L,R. \tag{35}$$

Finally, from Eqs. (32)–(35), one can obtain

$$\rho(x)_L = \frac{\alpha}{1+\alpha} + \frac{\beta(1-\alpha)^2}{(1+\alpha)(\alpha+\beta-2\alpha\beta)}x, \quad 0 < x \le 1, \tag{36}$$

and

$$\rho(x)_R = \frac{\beta}{1+\beta} + \frac{\beta(1-\alpha)(1-\beta)}{(1+\beta)(\alpha+\beta-2\alpha\beta)} + \frac{\alpha(1-\beta)^2}{(1+\beta)(\alpha+\beta-2\alpha\beta)}(x-1), \quad 1 < x \le 2. \tag{37}$$

The densities for these boundary conditions can be calculated as $\rho(x=0)_L = \alpha/(1+\alpha)$ and $\rho(x=2)_R = 1/(1+\beta)$. These results are completely identical with the theoretical analysis in Refs. [37,38]. At the junction point N, the densities are equal to $\rho(x=1)_L = [\alpha^2(1-\beta)+\beta(1-\alpha)]/[(1+\alpha)(\alpha+\beta-2\alpha\beta)]$, $\rho(x=1)_R = \beta(1-\alpha\beta)/[(1+\beta)(\alpha+\beta-2\alpha\beta)]$. Note that, on the transition line between the (LD, LD) and (HD, HD) phases, we obtain the relationship $\alpha = \beta/[m+(m-1)\beta]$.

IV. SIMULATION RESULTS AND DISCUSSIONS

To validate our theoretical analysis, computer simulations are conducted. Here, we present only a synchronous TASEP with a Y-type junction, that is, $m=2$. The numbers of sites of the subchains and the main chain are all equal to 1000. In simulations, stationary density profiles are obtained by averaging 10^8 sampling at each site. The first $10^5 N$ time steps are discarded as transients.

The density profiles for the (LD, LD), (HD, HD) and (HD, MC) phases are shown in Fig. 4. We only illustrate the density properties of subchain 1 and the main chain since the density properties of the other subchain are essentially the same as subchain 1. It is found that there is good agreement between Monte Carlo simulations (MCS) and mean-field analysis (MFA) [see Figs. 4(a)–4(e)], which verifies our theoretical investigations.

The phenomenological domain wall (DW) theory developed in Sec. III is used to calculate the density profiles of phase boundaries such those of the (LD, HD) and (LD, MC) phases (see Fig. 5). The results obtained from the domain wall theory show agreement with the computer simulations. When α and β both increase and also maintain $\alpha = \beta/[m+(m-1)\beta]$, the system remains in the (LD, HD) phase until $\beta=1$; the slopes of the density profiles for $x<1$ decrease until the slope is reduced to 0.5, while the slopes of the density profiles for $1<x<2$ also decrease until the slope decreases to 0. For instance, the slope decreases from 0.588 to 0.542 [also see Eq. (32)] when α increases from 0.1 to 0.2 [see Figs. 5(a) and 5(b)]. Finally, the slopes of the density profiles of the subchains become 0.5 and the slope of the density profile of the main chain becomes 0 when $\alpha=1/3$ and $\beta=1$ [see Fig. 5(c)]. Additionally, Monte Carlo simulations, theoretical calculations, and domain wall theory all show that, when $\alpha=1/3$ and $\beta=1$ (i.e., in the transition phase between the other four phases), the main chain is in the maximal current phase.

The density profiles of the systems for $m=2$ and 3 with a synchronous update scheme are simulated and compared (see Fig. 6). According to Eq. (7), the phase boundary between the (LD, LD) and (HD, HD) phases can be described as $\alpha = \beta/(2+\beta)$ for $m=2$ and $\alpha = \beta/(3+2\beta)$ for $m=3$. Figure 6

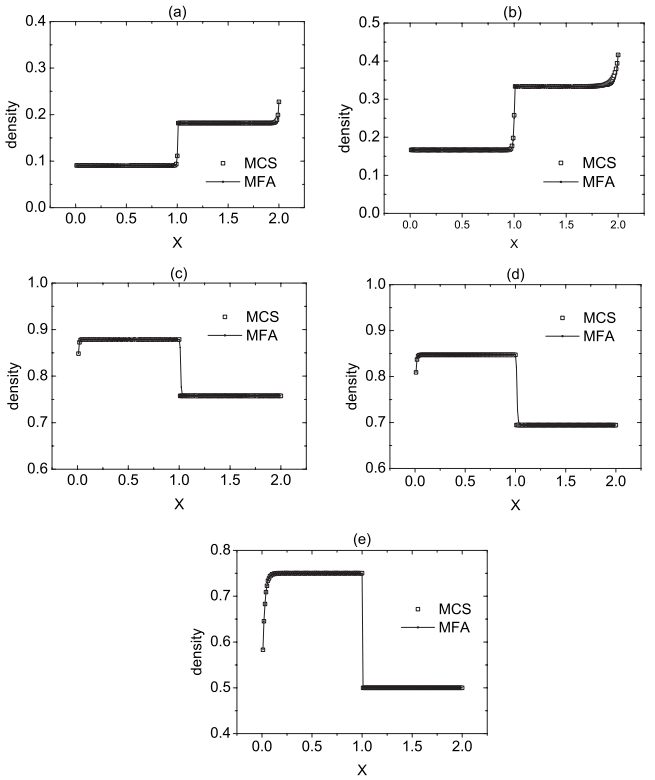

FIG. 4. Density profiles obtained from our theoretical calculations and Monte Carlo simulations when $m=2$: (a), (b) (LD, LD), (c), (d) (HD, HD), and (e) (HD, MC) phase. The parameters are (a) $\alpha=0.1$ and $\beta=0.8$, (b) $\alpha=0.2$ and $\beta=0.8$, (c) $\alpha=0.8$ and $\beta=0.32$, (d) $\alpha=0.8$ and $\beta=0.44$, and (e) $\alpha=0.6$ and $\beta=1.0$.

shows that both systems are in the (LD, LD) phase when $\alpha=0.1$ and $\beta=0.8$. However, when α increases (e.g., $\alpha=0.2$), the system for $m=2$ is still in the (LD, LD) phase, while the system for $m=3$ is in the (HD, HD) phase [see Fig. 6(b)]. This is because the phase boundary between the (LD, LD) and (HD, HD) phases moves toward the left when m increases [see Fig. 2(a)]. Density profiles in the (HD, HD) phase for both $m=2$ and 3 are shown in Fig. 6(c). Compared with Figs. 6(a) and 6(c), it can be seen that the density profiles of the subchains of both systems are the same when both systems are in the (LD, LD) phase, while the density profiles of the main chains of both systems are the same when both systems are in the (HD, HD) phase. Figure 6(d) illustrates that the system is in the (LD, LD) phase for $m=2$, while it is in the (HD, MC) phase for $m=3$.

We can also see the similarities and differences between the phase diagram of the system with the synchronous or parallel update scheme [see Fig. 2(b)] and that of the system with the random update scheme (see Fig. 3 in [23]). One can see that the structures of the phase diagrams are similar. All have five phases. Also, an increase in the number of subchains (i.e., inputs) only shifts the transition line between the (LD, LD) phase and the (HD, HD) phase, which does not fall on the boundaries of the phase diagrams. However, the differences in the phase diagrams include the following: (i) The (HD, MC) phase region in the phase diagram of the system with the random update scheme is reduced to a line in that of the system with the synchronous update scheme; and (ii) the

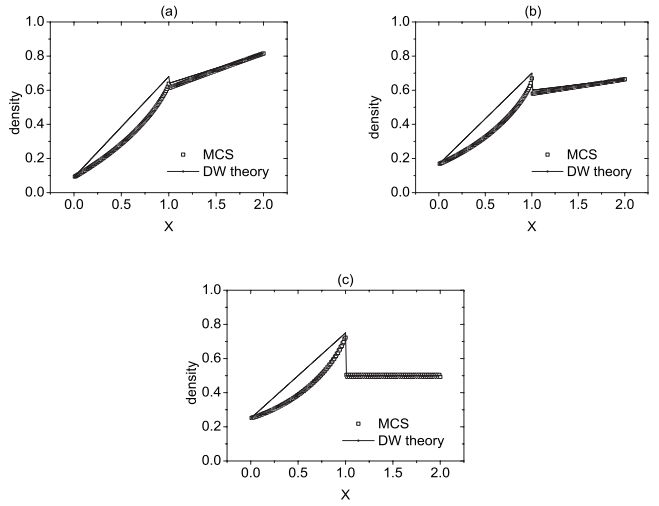

FIG. 5. Density profiles obtained by the domain wall theory and Monte Carlo simulations when $m=2$: (a), (b) phase coexistence line between the (LD, LD) and (HD, HD) phases, and (c) coexistence lines between the (LD, LD), (LD, HD), (HD,HD), and (HD, MC) phases. The parameters are (a) $\alpha=0.1$ and $\beta=0.222$, (b) $\alpha=0.2$ and $\beta=0.5$, and (c) $\alpha=1/3$ and $\beta=1.0$.

line of the (LD, MC) phase in the phase diagram of the system with the random update scheme is reduced to a point in the phase diagram of the system with the synchronous update scheme.

Figure 7 shows the differences in the density profiles of the systems with the synchronous update scheme and that with the random update scheme when $m=2$. In Fig. 7(a), these two systems are in the (LD, LD) phase when $\alpha=0.1$ and $\beta=0.8$. When α is increased to 0.2 and β is unchanged, the system with the synchronous update scheme is still in the (LD, LD) phase, while the phase of the system with the random update scheme changes to the (HD, MC) phase [see Fig. 7(b)]. Figure 7(c) shows both systems in the (HD, HD) phase when $\alpha=0.8$ and $\beta=0.32$. With increase of β (e.g., to

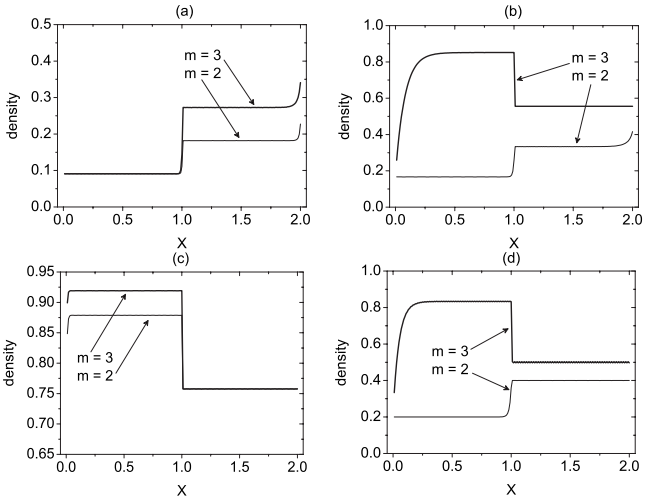

FIG. 6. Density profiles in Monte Carlo simulations when $m=2$ and 3. The parameters are (a) $\alpha=0.1$ and $\beta=0.8$, (b) $\alpha=0.2$ and $\beta=0.8$, (c) $\alpha=0.8$ and $\beta=0.32$, and (d) $\alpha=0.25$ and $\beta=1.0$.

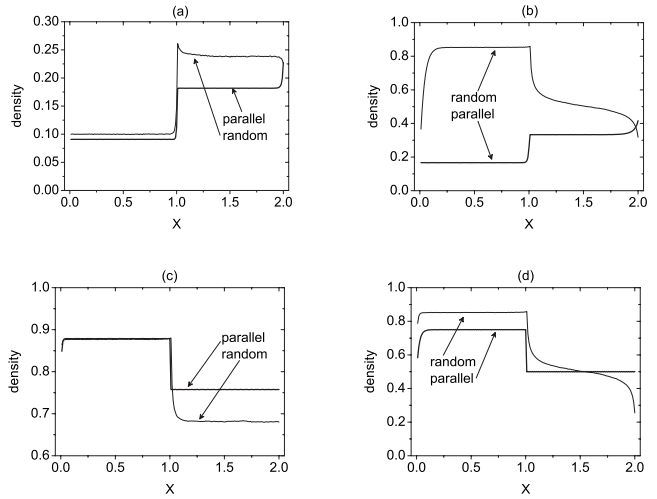

FIG. 7. Density profiles in Monte Carlo simulations when $m=2$ with random and parallel updates. The parameters are (a) $\alpha=0.1$ and $\beta=0.8$, (b) $\alpha=0.2$ and $\beta=0.8$, (c) $\alpha=0.8$ and $\beta=0.32$, and (d) $\alpha=0.8$ and $\beta=0.8$.

$\beta=0.8$), the phase of the system with the random update scheme changes to the (HD, MC) phase, while the other system stays in the (HD, HD) phase (see Fig. 7(d)).

Note that the system also exhibits a particle-hole symmetry, since forward movement of particles at junction points is equivalent to backward movement of holes with the same priority. Also, our method can be used to analyze synchronous TASEPs with a single–input–multiple-output junction. Other inhomogeneous synchronous TASEPs can be investigated in a similar way. For instance, it would be interesting to study a MISO junction where these parallel subchains are dynamically different.

V. SUMMARY AND CONCLUSIONS

Multiple-input–single-output junctions are relevant to many biological processes as well as vehicular and pedestrian traffic flow. Synchronous totally asymmetric exclusion processes with a MISO junction are investigated in this paper. Theoretical solutions, the mean-field approximation, and domain wall theory are developed. Extensive computer simulations are conducted. Our theoretical analysis suggests that there are five possible stationary phases [(LD, LD), (LD, HD), (LD, MC), (HD, HD), and (HD, MC)]. The (LD, HD) phase corresponds to the transition line {when $\alpha=\beta/[m+(m-1)\beta]$ and $\beta<1$, where m is the number of subchains} between the (LD, LD) and the (HD, HD) phases. The (LD, MC) phase [when $\alpha=1/(2m-1)$ and $\beta=1$] is the transition phase between the (LD, LD), (LD, HD), (HD, HD), and (HD, MC) phases. Also, the non equilibrium stationary state, the stationary-state phases, and the phase boundaries are determined by the boundary conditions of the system as well as by the number of subchains. The phase boundary moves to the left in the phase diagram when the number of subchains increases. The density profiles are simulated and show good agreement with the theoretical analysis.

We also compare the phase diagrams and density profiles between the systems with synchronous and random update schemes. The main differences in the phase diagrams include the following. (i) The (HD, MC) phase region in the phase diagram of the system with the random update scheme reduced to a line in that of the system with the synchronous update scheme; and (ii) the line of the (LD, MC) phase in the phase diagram of the system with the random update schemes reduced to a point in the phase diagram of the system with the synchronous update scheme.

The approach used in this paper can be used directly to analyze TASEPs with a single-input–multiple-output junction in a parallel updating procedure.

ACKNOWLEDGMENTS

The authors gratefully acknowledge the comments and suggestions of the anonymous reviewers, which helped in improving the clarity and the quality of the paper. R.W. acknowledges the support of the Massey University Research Fund and Massey University International Visitor Research Fund. R.J. was supported by the National Basic Research Program of China (Grant No. 2006CB705500), the NNSFC under Project Nos. 10532060, 70601026, and 10672160, the CAS President Foundation, the NCET, and the FANEDD.

[1] D. Helbing, Rev. Mod. Phys. **73**, 1067 (2001).
[2] D. Chowdhury, A. Schadschneider, and K. Nishinari, Phys. Life. Rev. **2**, 318 (2005).
[3] T. Chou, Phys. Rev. Lett. **80**, 85 (1998).
[4] L. B. Shaw, R. K. P. Zia, and K. H. Lee, Phys. Rev. E **68**, 021910 (2003)
[5] G. M. Schütz, Europhys. Lett. **48**, 623 (1999).
[6] B. Widom, J. L. Viovy, and A. D. Defontaines, J. Phys. I **1**, 1759 (1991).
[7] S. Klumpp and R. Lipowsky, J. Stat. Phys. **113**, 233 (2003).
[8] D. Chowdhury, L. Santen, and A. Schadschneider, Phys. Rep. **329**, 199 (2000).
[9] A. John, A. Schadschneider, D. Chowdhury, and K. Nishinari, J. Theor. Biol. **231**, 279 (2004).
[10] B. Derrida, Phys. Rep. **301**, 65 (1998).
[11] G. M. Schütz, in *Phase Transitions and Critical Phenomena*, edited by C. Domb and J. L. Lebowitz (Academic Press, San Diego, 2001), Vol. 19.
[12] R. Lipowsky, S. Klumpp, and T. M. Nieuwenhuizen, Phys. Rev. Lett. **87**, 108101, (2001).
[13] S. Klumpp and R. Lipowsky, Europhys. Lett. **66**, 90, (2004).
[14] A. Parmeggiani, T. Franosch, and E. Frey, Phys. Rev. Lett. **90**, 086601 (2003); Phys. Rev. E **70**, 046101 (2004).
[15] V. Popkov, A. Rákos, R. D. Willmann, A. B. Kolomeisky, and G. M. Schütz, Phys. Rev. E **67**, 066117 (2003).
[16] N. Mirin and A. B. Kolomeisky, J. Stat. Phys. **110**, 811

(2003).
[17] M. R. Evans, R. Juhász, and L. Santen, Phys. Rev. E **68**, 026117 (2003).
[18] R. Juhász and L. Santen, J. Phys. A **37**, 3933 (2004).
[19] S. Mukherji and S. M. Bhattacharjee, J. Phys. A **38**, L285 (2005).
[20] K. Nishinari, Y. Okada, A. Schadschneider, and D. Chowdhury, Phys. Rev. Lett. **95**, 118101 (2005).
[21] T. Mitsudo and H. Hayakawa, J. Phys. A **39**, 15073 (2006).
[22] E. Pronina and A. B. Kolomeisky, J. Phys. A **37**, 9907 (2004); **40**, 2275 (2007).
[23] E. Pronina and A. B. Kolomeisky, J. Stat. Mech.: Theory Exp. (2005) P07010.
[24] T. Mitsudo and H. Hayakawa, J. Phys. A **38**, 3087 (2005).
[25] E. B. Stukalin and A. B. Kolomeisky, Phys. Rev. E **73**, 031922 (2006).
[26] T. Reichenbach, T. Franosch, and E. Frey, Phys. Rev. Lett. **97**, 050603 (2006).
[27] R. Jiang, R. Wang, and Q. S. Wu, Physica A **375**, 247 (2007).
[28] R. Wang, M. Liu, and R. Jiang, Physica A **387**, 457 (2008).
[29] S. Klumpp and R. Lipowsky, Phys. Rev. E **70**, 066104 (2004).
[30] P. Pierobon, M. Mobilia, R. Kouyos, and E. Frey, Phys. Rev. E **74**, 031906 (2006).
[31] D. Chrétien, F. Metoz, F. Verde, E. Karsenti, and R. H. Wade, J. Cell Biol. **117**, 1031 (1992).
[32] M. A. Burack, M. A. Silverman, and G. Banker, Neuron **26**, 465 (2000).
[33] L. S. B. Goldstein, Proc. Natl. Acad. Sci. U.S.A. **98**, 6999 (2001).
[34] D. D. Hurd and W. M. Saxton, Genetics **144**, 1075 (1996).
[35] D. Helbing, R. Jiang, and M. Treiber, Phys. Rev. E **72**, 046130 (2005).
[36] A. B. Kolomeisky, G. M. Schütz, E. B. Kolomeisky, and J. P. Straley, J. Phys. A **31**, 6911 (1998).
[37] L. G. Tilstra and M. H. Ernst, J. Phys. A **31**, 5033 (1998).
[38] J. de Gier and B. Nienhuis, Phys. Rev. E **59**, 4899 (1999).